https://doi.org/10.5194/acp-2020-1252
Preprint. Discussion started: 18 January 2021

Atmospheric Chemistry and Physics Discussions

Satellite retrieval of cloud base height and geometric thickness of low-level cloud based on CALIPSO

Xin Lu[1], Feiyue Mao[1, 2, 3], Daniel Rosenfeld[1, 4], Yannian Zhu[5, 6, *], Zengxin Pan[4], Wei Gong[1, 7]

[1]State Key Laboratory of Information Engineering in Surveying, Mapping, and Remote Sensing, Wuhan University, Wuhan, 430079, China
[2]School of Remote Sensing and Information Engineering, Wuhan University, Wuhan, 430079, China
[3]Collaborative Innovation Center for Geospatial Technology, Wuhan, 430079, China
[4]Institute of Earth Sciences, The Hebrew University of Jerusalem, Jerusalem, 91904, Israel
[5]School of Atmospheric Sciences, Nanjing University, Nanjing, 210023, China
[6]Joint International Research Laboratory of Atmospheric and Earth System Sciences & Institute for Climate and Global Change Research, Nanjing University, Nanjing, 210023, China
[7]Electronic Information School, Wuhan University, Wuhan, 430072, China

Correspondence to: Yannian Zhu (yannianzhu@gmail.com)

Abstract.

Lidar-based measurements of cloud base and top height (CBH and CTH) and cloud geometrical thickness (CGT) with greatly improved accuracy provide new scientific insights. However, direct observation of the active Cloud Aerosol Lidar and Infrared Pathfinder Satellite Observation (CALIPSO) cannot penetrate optically thick clouds to their base. A work around for this problem is developed and validated in this study. This method is based on the 333-m resolution low-level water cloud data obtained from the Vertical Feature Mask product of CALIPSO. The methodology can effectively minimize the interference of surface signals, boundary layer aerosols and cloud anvils of CBH retrieval. The methodology overcomes the full attenuation of the lidar in optically thick clouds by assuming that CBH of boundary layer clouds is similar over an area of several tens of km. This allows taking the CBH of the neighbouring penetrable shallower cloud as having CBH representative for the entire cloud field. The retrieved CBH was validated against two surface-based ceilometer measurements in the islands of Barbados and the Azores, with an error standard deviation of ±100 m. The accurate CBH allow us to obtain CGT, which is an essential parameter in understanding of the aerosol-cloud interaction. Based on this newly developed methodology, we retrieved the annual, seasonal and diurnal distributions of global CBH, CTH and CGT for two years, and analysed the variations of CBH and CTH over the ocean and land.

Some highlights from these first of a kind high-precision cloud geometry observations show for annual mean values that: (1) The lowest CBH occurs over the eastern margins of the subtropical oceans and increases westward from 300-400 to 700-800 m. The CGT increases from 300 to 1200 m, respectively. In the western part of the tropical oceans CBH is 500-600 m and CGT is ~1500 m. (2) A narrow band of lower CBH and CGT occurs over the Equator, especially over the eastern parts of the oceans. (3) CBH and CGT over the Amazon and Congo rain forests are 1200 and 1500 m, respectively. CBH over the drier tropical lands is 1500-2000 m, with CGT of 800-1000 m. (4) Lowering CBH towards Antarctica in the Southern Oceans, while

https://doi.org/10.5194/acp-2020-1252
Preprint. Discussion started: 18 January 2021

Atmospheric Chemistry and Physics Discussions

deepening CGT. (5) Seasonally, the mid-latitude global oceans have the lowest CBH (mostly below 500 m) and CGT in summer seasons, and the highest cloud in winter, while the CBH and CGT distribution reversed over high-latitude Southern Oceans. (6) There is an obvious diurnal cycle of maximum CTH and CGT over the tropics. Over the ocean, there is no discernible diurnal cycle in CBH, but during night CTH is higher by ~300 m.

1 Introduction

Satellite retrievals of cloud base height (CBH), cloud top height (CTH) and cloud geometrical thickness (CGT) are essential for quantifying cloud dynamic and microphysical properties and aerosol-cloud interactions (Fan et al., 2016;Fan et al., 2020). Atmospheric aerosols act as cloud condensation nuclei (CCN) play a crucial role in the formation of size and concentration of cloud droplets and regulate the radiation balance of the Earth-atmosphere system (Rosenfeld et al., 2019). Satellite retrieval of CCN depends on the cloud base updraft (Rosenfeld et al., 2016;Efraim et al., 2020;Zheng, 2019), which is linearly related to CBH (Zheng and Rosenfeld, 2015;Zheng et al., 2020). The combination of cloud base updraft and CCN determines cloud base droplet concentration (N_d), which in turn determines the cloud's albedo for a given liquid water path (Twomey, 1974;Sato and Suzuki, 2019). However, the current satellite-retrieved N_d requires to assume an adiabatic fraction (f_{ad}) of the cloud water, which is usually taken as f_{ad} =1 (Grosvenor and Wood, 2014). In reality, f_{ad} is often much smaller than 1, which leads to a serious underestimation relative to the in situ measured N_d (Efraim et al., 2020). Therefore, accurate CBH and CGT are extremely important to reduce the uncertainty of aerosol-cloud interaction.

CTH is crucial to provide the three-dimensional structure information of cloud liquid water content (Huo et al., 2020). Also CBH has practical significance for the aviation community (Noh et al., 2017). It was shown recently that CGT can isolate the aerosol-cloud interaction from much of the influence of meteorology (Rosenfeld et al., 2019;Sato and Suzuki, 2019). CBH and CTH are fundamental cloud properties that are required to be parameterized correctly for improving model simulations of climate and climate change (Grosvenor et al., 2017;Zhao and Suzuki, 2019;Lenaerts et al., 2020). Therefore, it is necessary to obtain the accurate CBH and CTH and further retrieve CGT. All these properties are important to understand the complex cloud microphysical processes and aerosol-cloud interaction (Stephens and Webster, 2010;Dupont et al., 2011;Kyle et al., 2016).

Satellites provide a wide-range of cloud observations from space (Stephens et al., 2019). It is feasible to retrieve CTH based on satellite data because satellite can observe the cloud top directly (Weisz et al., 2007). Retrieval of CBH is much more challenging, but necessary for retrieving CGT. There are already many different methods to retrieve the CBH based on different satellite observation data. The Suomi National Polar-orbiting Partnership (Suomi NPP) Visible Infrared Imaging Radiometer Suite (VIIRS) is based on the CTH and CGT to retrieve the CBH, and the CGT is calculated using the ratio of the cloud water path to the cloud water content, which requires to assume f_{ad} = 1 (Baker, 2011). To investigate the accuracy of VIIRS CBH retrieval algorithm, Seaman et al. (2017) compared the CBH from the VIIRS with those from the CloudSat cloud profile radar, and showed that because the VIIRS retrieval algorithm is insensitive to upper clouds, the CBH error for all clouds in global is

https://doi.org/10.5194/acp-2020-1252
Preprint. Discussion started: 18 January 2021


Atmospheric Chemistry and Physics Discussions

3.7 km, and even for clouds with accurate CTH, the root-mean-square error (RMSE) of CBH reaches 2.3 km. Böhm et al. (2019) retrieved global CBH data based on multi-angle satellite data, and the validation results based on ground-based observations showed that the RMSE of CBH obtained by this method was ~400 m. Li et al. (2013) conducted the retrieval of global marine boundary layer CBH based on boundary layer lapse rate observation from the A-train satellite constellation, and the standard deviation of the CBH obtained by this retrieval method from the CBH of CloudSat is 540 m. Zhu et al. (2014) used the imager of the Suomi NPP VIIRS and retrieved cloud base of convective clouds at an accuracy of 200 m, but this retrieval relied on strong contrast between the cloud and underlying surface brightness, and could not work at night. It can be seen that these CBH retrieval methods either have low accuracy or do not provide all-day CBH data. Therefore, there is a yet unfulfilled scientific need to obtain high-precision all-day CGT/CBH based on active satellite observations.

Satellite lidars, such as the Cloud Aerosol Lidar and Infrared Pathfinder Satellite Observation (CALIPSO), have a good potential for retrieval of CBH (Winker et al., 2009). However, CALIPSO typically provides only CBHs for thin clouds, because it can penetrate only clouds with optical thickness of less than 5 (Mace and Zhang, 2014). When the thickness of the cloud is sufficient to fully attenuate the CALIPSO lidar signal, CALIPSO cannot provide information about the base of these clouds. Mülmenstädt et al. (2018) attempted to retrieve the global CBH using CALIPSO Vertical Feature Mask (VFM) data and evaluated the retrieval algorithm based on ground-based ceilometer observation, which provided the basic idea to retrieve the high-precision CGT, but the overall RMSE of CBH exceeded 500 m. There are many other challenges. For example, strong surface echoes can affect the identification of cloud bases of CALIPSO observations (Burton et al., 2013). In addition, due to the influence of the aerosol, which are abundant in the boundary layer, the low-level cloud may be masked by dense aerosol layers, thereby affecting the determination of the cloud layer (Vaughan et al., 2005). Further, large areas of elevated cloud layers can also interfere with the CBH retrieved by active CALIPSO observations. These factors lead to a large uncertainty in the typical CBH obtained directly based on CALIPSO observations.

To solve the above problems, we proposed in this study a new methodology by using the highest resolution of CALIPSO measurements to retrieve the global CBH, CTH and CGT of low-level clouds and validate against in situ ceilometer measurement. These low-level clouds reflect most of the incident solar radiation received by the Earth back into space, and they are of great interest for various applications (such as retrieval of cloud microphysical properties, weather prediction and so on). Therefore, high-precision CBH and CGT data of low-level clouds are the foundation to the follow-up aerosol-cloud interaction research. The data used in this study are presented in Section 2 and the retrieval method is given in Section 3. The CALIPSO-retrieved CBHs were validated against in situ ceilometer measurements in Section 4. Based on the validated-CBH, CTH and CGT were retrieved globally and used for producing global annual, seasonal and diurnal distributions maps of CBH, CTH and CGT in Section 5. Several features are further discussed in Section 6 based on this high-precision cloud geometry information. Conclusions are provided in Section 7.

https://doi.org/10.5194/acp-2020-1252
Preprint. Discussion started: 18 January 2021


Atmospheric Chemistry and Physics Discussions

2 Data

2.1 CALIPSO VFM data

The satellite data we analyzed in this study are from the Cloud Aerosol Lidar with Orthogonal Polarization (CALIOP) lidar on CALIPSO satellite, which can provide two-dimensional (vertically and horizontally along the satellite track) information of clouds with a global coverage (Winker et al., 2007). The cloud top and base can be obtained from the CALIOP VFM product (Winker et al., 2009). For each CALIOP attenuated backscattering profile, the VFM product identifies features classified as clouds, aerosols, stratospheric features, and surfaces; this is known as feature type. Moreover, the VFM also provides the thermodynamic phase of cloud layers (water cloud, ice cloud) and horizontal resolution that the retrieval was based on. The CALIOP retrieval algorithm must average over a horizontal distance to collect sufficient signal that allows the identification of features on the background noise of atmospheric molecules scattering. In this study, we use VFM version 4.10 data for the full years of 2014 and 2017. The VFM files are available from ASDC (https://eosweb.larc.nasa.gov/).

2.2 Ground validation data

The retrieval algorithm is validated by ceilometer observations, which are lidar measurements done looking from the surface upward towards cloud base. Since much of the low-level cloud occurs over the ocean, we used ceilometer sites on islands at different latitudes to validate the CALIPSO-retrieved CBH. One site is at low latitude and one at mid latitude. The low latitude site is Barbados (13.2° N, 59.4° W; Barbados Cloud Observatory, Germany, https://barbados.mpimet.mpg.de/). The mid latitude site is the Eastern North Atlantic (ENA) site located at the Azores (39.1° N, 28.0° W; Atmospheric Radiation Measurement, https://www.arm.gov/data). Figure 1 gives the schematic of data matching between CALIPSO and the ceilometer site. To obtain the CALIPSO-retrieved CBH that matches the ceilometer-measured CBH, a scene of 1° is selected (the gray shade area in Figure 1), centered in time on the overpass time and extending 0.5° to the left and right along the CALIPSO track. The scene is selected if the distance from the CALIPSO center point to the ceilometer site is less than 150 km, and is used for matching the CALIPSO with the ceilometer data.

https://doi.org/10.5194/acp-2020-1252
Preprint. Discussion started: 18 January 2021

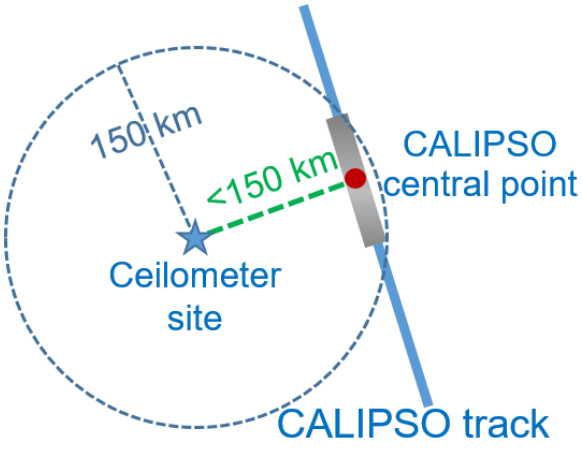

Figure 1: Schematic of matching between the CALIPSO and the ceilometer observation site. The blue pentagram indicates the location of ceilometer site, the blue solid line is the CALIPSO track, the red solid circle represents the CALIPSO central point, the dashed green line represents the shortest distance from the ceilometer site to the CALIPSO central point, and the grey shade area is the 1° CALIPSO scene. The blue circle is centered on the ceilometer site and has a radius of 150 km.

The retrieval methodology in this study relies on the assumption of the undisturbed boundary layer with a similar cloud base height within the scene. The topography of the islands at the Azores has volcanic peaks with heights up to 500 m, and may violate the homogeneity assumption. To avoid the anomalous uplift of clouds by the topography of these adjacent islands, we restricted the CALIPSO data according to the terrain and wind directions as showed in Figure A1. If the elevation corresponding to the CALIPSO data matching the ENA site ceilometer data is higher than 30 m, the CALIPSO data are rejected. Similarly, to avoid the situation that the clouds traveled above the adjacent islands were perturbed, we rejected the CALIPSO data with wind direction of southwest/southeast if the CALIPSO track is located at the east/west ocean of ENA site (Figures A1a and A1b). The wind direction is from the meteorological observation data of ENA site, and the elevation data are from the CALIPSO VFM product.

3 CALIPSO CGT retrieval algorithm

The objective of CBH retrieval is to retrieve the forming level of the clouds. In the case of a well-mixed boundary layer it is the lifting condensation level. When clouds are decoupled, that level is usually higher. That formative cloud base level is similar in areas with similar thermodynamic structure, which is conducive to a nearly constant cloud base height. The retrieval algorithm relies on this assumption, by adopting the lowest reliably detected cloud height along a CALIPSO track of approximately 100 km (1° along the track) as the cloud base height.

https://doi.org/10.5194/acp-2020-1252
Preprint. Discussion started: 18 January 2021

Atmospheric Chemistry and Physics Discussions

3.1 Extraction of 333-m horizontal resolution low-level cloud feature

In this study we retrieve CBH and CGT of CALIPSO VFM scenes that identified low-level water clouds. Low clouds are defined following the International Satellite Cloud Climatology Project as clouds distributed below 680 hPa (Hahn et al., 2001), which also complies with the detection range of the ceilometer. Figure 2 displays an example of CALIPSO low-level cloud feature determination. For each 1° scene along the CALIPSO track, the distribution of the low-level water clouds which had sufficient signal to be detected with a horizontal resolution of 333-m (light blue areas in Figure 2c) was obtained. These cloud features were identified based on the CALIPSO feature type data (Figure 2a) and resolution data (Figure 2b). Then, based on the low-level cloud information in Figure 2c, we could retrieve the CBH, CTH and CGT of this scene.

Using 333-m resolution cloud feature information allows a better separation between the clouds and boundary layer aerosols, because the aerosol identification is based mostly on 1-km or lower resolution data, as evident in Figure 2b (Vaughan et al., 2005). Moreover, CBH obtained from higher resolution VFM data was closer to the CBH that retrieved from MODIS based on adiabatic hypothesis (Seung-Hee et al., 2017). Also, low horizontal resolution is most likely to lead to false detection of clouds (Mace and Zhang, 2014). Therefore, it is more reliable to use the water cloud information with a resolution of 333-m to retrieve the CBH of low-level clouds than other horizontal resolutions. Thus, we chose to use 333-m resolution instead of other resolutions for CBH and CGT retrieval.

https://doi.org/10.5194/acp-2020-1252
Preprint. Discussion started: 18 January 2021

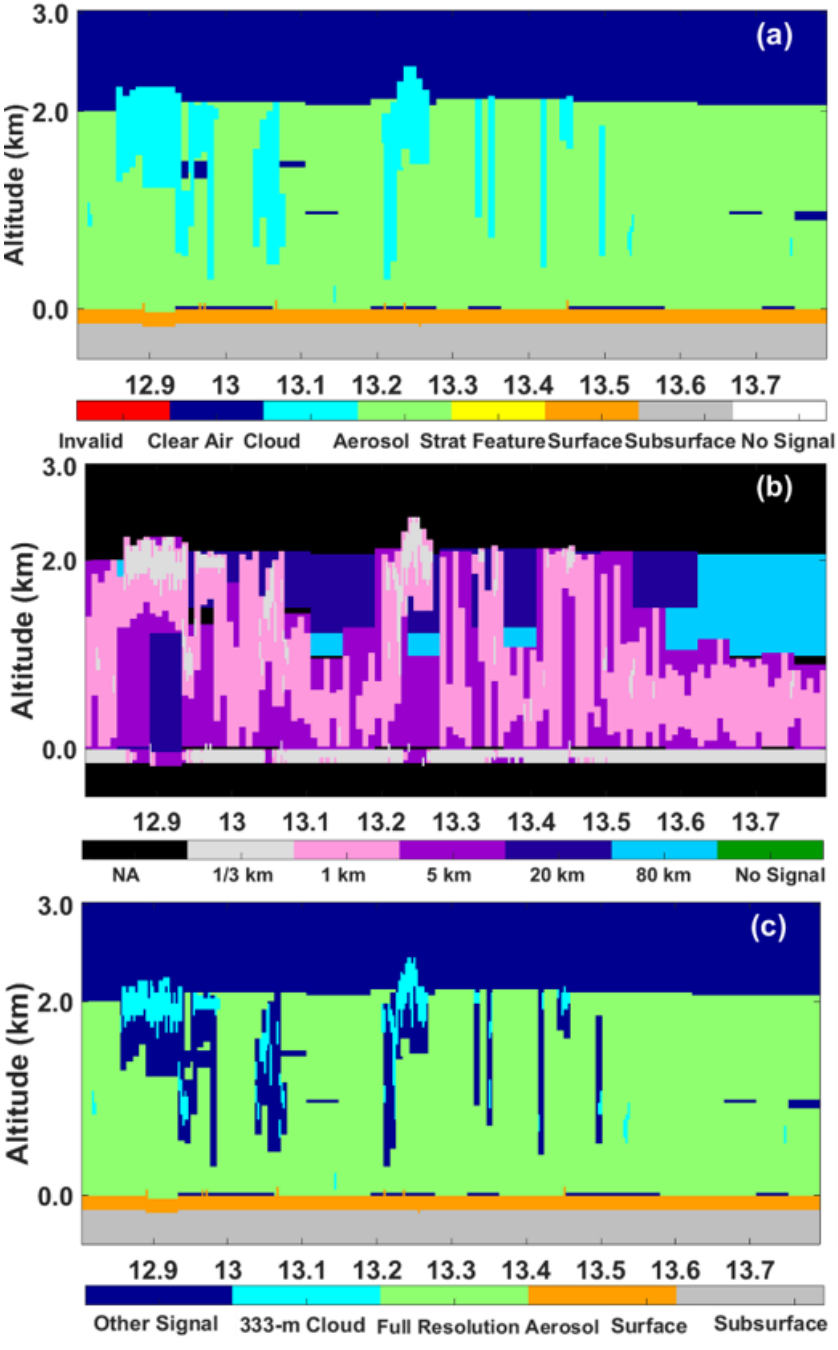

Figure 2: Schematic of CALIPSO low-level cloud feature determination (CALIPSO VFM data at (UTC) 05:51:17 on 3 January 2017). (a) Latitude-altitude distribution of feature type based on CALIPSO VFM feature type parameter, the light blue areas represent the water cloud features. (b) Resolution information distribution based on CALIPSO VFM resolution parameter, the light blue areas represent the 333-m resolution features. (c) 333-m horizontal resolution water cloud distribution combined by (a) and (b); the light blue areas indicate the 333-m horizontal resolution water clouds, the green areas refer to aerosols at any resolution, the orange area is the surface.

https://doi.org/10.5194/acp-2020-1252
Preprint. Discussion started: 18 January 2021

Atmospheric Chemistry and Physics Discussions

3.2 Optically thick clouds

CALIPSO lidar can penetrate fully and detect the cloud base only in clouds with optical thickness < ~5 (Mace and Zhang (2014). However, we also need to obtain the base height of optically thick clouds, which are widespread in the atmosphere and important objects for aerosol-cloud interaction research. In this study, we follow a main hypothesis that, within a given area (1° scene), the cloud forming height, which is the lifting condensation level of coupled clouds, is approximately homogeneous within an air mass. Thus, CBH retrieved by CALIPSO lidar signal for the thin cloud is a good proxy for the CBH of an entire cloud field, especially for the optically thicker clouds within the field (optical thickness >5; Mülmenstädt et al. (2018)).

3.3 CALIPSO initial CBH in 1° scene

For each 1° scene along the CALIPSO track, based on 333-m horizontal resolution low-level cloud information as described in Section 3.1, we obtained the height distribution of the lowest cloud feature (H_{min}) of each water cloud profile under which the surface is detectable as shown in Figure 3a. Then, based on this H_{min} data, we sort it from low H_{min} to high H_{min}, and obtained the H_{min} of each 10 % of quantiles in this 1° scene as shown in Figure 3b, which will be used to reduce the interference of strong surface signals and thick aerosols.

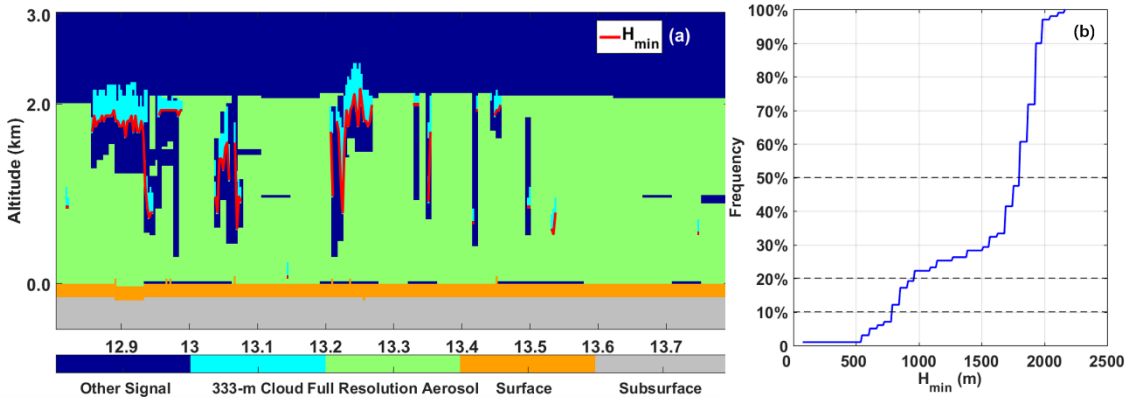

Figure 3: (a) The same as Figure 2c but with the distribution of H_{min} (the red line). (b) Cumulative distribution of the H_{min} at any quantile for the scene in Figure 3a (The black dotted lines represent the H_{min} at the 10 %, 20 %, and 50 % quantile, respectively.).

In order to decrease the effect of extremely low H_{min}, caused by mixture of surface signals and cloud features or VFM misclassified near surface thick aerosols as clouds (Burton et al., 2013;Vaughan et al., 2005), the lowest height of H_{min} cannot be used as the initial CBH of this 1° scene. In order to obtain the optimal quantile of the initial CBH, we carried out a sensitivity test based on the CALIPSO-retrieved CBH and the ceilometer-measured CBH from two ground observation stations (Barbados site and ENA site) in 2017 as showed in Figure 4. Taking a 1° scene along the CALIPSO track, which the center point to the ceilometer observation station within a distance of 150 km, we obtained the CB_{ceilo}, which refers to the distribution of the base height of the cloud features observed by ceilometers. Then, the lowest 10 % quantile of the CB_{ceilo} within 30 minutes before and after the CALIPSO overpass time is determined as true CBH. The sensitivity test shows that the application of CALIPSO

https://doi.org/10.5194/acp-2020-1252
Preprint. Discussion started: 18 January 2021

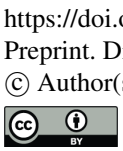

Atmospheric Chemistry and Physics Discussions

H_{min} at 10 % quantile as the initial CBH of this 1° scene greatly reduces the problem that the lowest H_{min} retrieved from CALIPSO is much smaller than the true CBH (RMSE reduced by 22 m).

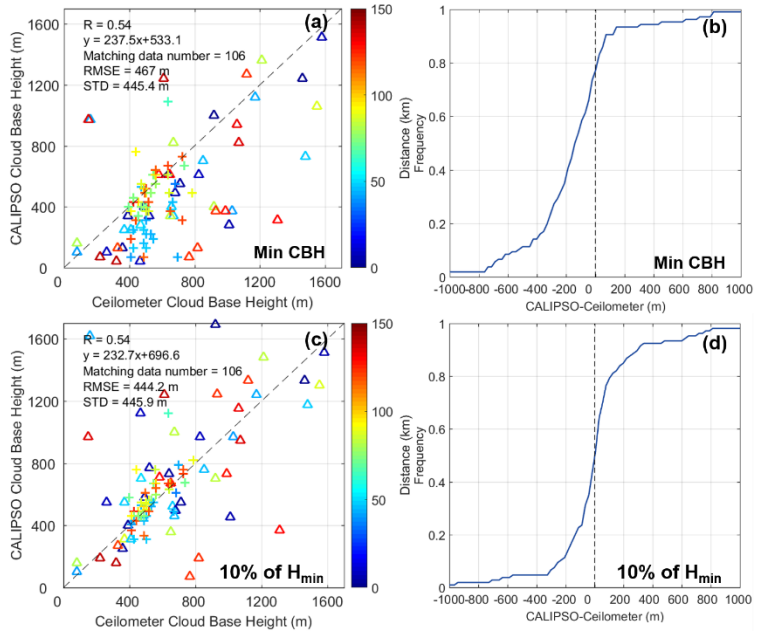

Figure 4: (a) Scatter plot of CALIPSO CBH (the minimum CBH for each 1° scene) and ceilometer CBH at two sites in 2017. The triangle represents the data for the ENA site, and the crosses represent the data for the Barbados site. The color represents the shortest distance from the CALIPSO ground track to the ceilometer site. (b) Cumulative distribution of the difference between CALIPSO CBH and Ceilometer CBH at two sites in 2017. (c)/(d) is the same as (a)/(b), but the CALIPSO CBH is at 10 % quantile of H_{min}.

3.4 Determination of CALIPSO CBH, CTH and CGT of 1° scenes

After getting the initial CBH (H_{min} at 10 % quantile), there are still many factors affecting the determination of the final CBH in the cloud scenes that contribute to the uncertainty or add limitations to the CBH retrieval. There are many confounding factors, including multilayer cloud fraction (F_{multi}), cloud cover (F_{cloud}), and detection efficiency of CALIOP lidar (E_{lidar}). These difficulties are overcome by the added selection criteria, which are tested against in situ ceilometer measurements as presented in the following sub-sections:

3.4.1 Multilayer clouds

Multilayer status of features can be detected by CALIPSO vertical profile measurements. In VFM data, for each profile (from the surface to the altitude of 20 km), if cloud features are continuous, then it is a profile with a single-layer cloud; if there is more than one cloud segment in that vertical profile, then this profile contains multilayer clouds. In this study, for each 1° CALIPSO scene, only profiles containing continuous single-layer clouds are used to retrieve CBH, CTH and their thickness, that is, any profile with multilayer clouds is excluded. This is because the aerosol-cloud interaction studies mainly focus on single-layer cloud. Therefore, when there are too many multilayer clouds in a 1° scene, in order to guarantee the effectiveness

https://doi.org/10.5194/acp-2020-1252
Preprint. Discussion started: 18 January 2021

Atmospheric Chemistry and Physics Discussions

of CBH retrieval, this scene will be rejected. We use the F_{multi} to represent the cloud cover of the multilayer clouds in the scene. For a given 1° CALIPSO scene, F_{multi} is calculated using Eq. (1):

$$F_{multi} = N_{multi}/N_{total}, \quad (1)$$

N_{multi} is the number of the CALIPSO lidar profiles that contains multilayer clouds, and N_{total} is the total number of the CALIPSO lidar profiles collected in that given 1° CALIPSO scene. In order to obtain the optimal threshold of F_{multi}, we carried out the sensitivity test as displayed in Figure 5. We can see that when F_{multi} < 40 %, the CALIPSO-retrieved CBH and ceilometer-measured CBH have the highest consistency (minimum RMSE, optimal linear correlation coefficient (R)). Therefore, when there are too many multilayer clouds in a scene (F_{multi} > 40 %), the scene is rejected.

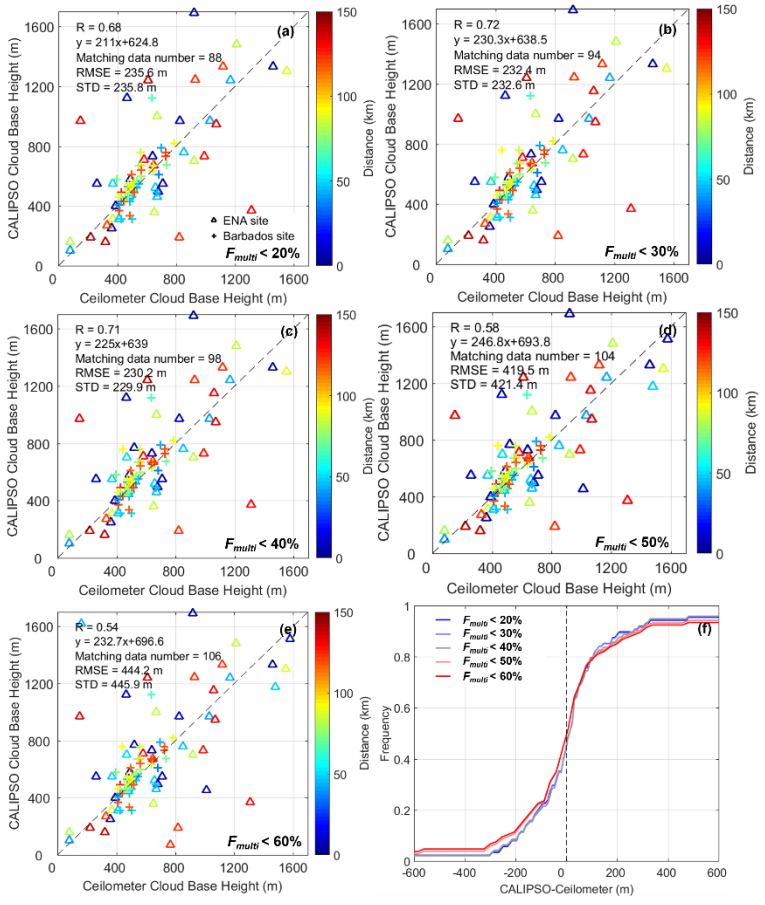

Figure 5: (a) Scatter plot of CALIPSO CBH (when multilayer cloud fraction (F_{multi}) of one scene is less than 20 %, we select this scene) and ceilometer-measured CBH at two sites in 2017. The triangle represents the data for the ENA site, and the crosses represent the data for the Barbados site. The color represents the shortest distance from the CALIPSO ground track to the ceilometer site. (b), (c), (d) and (e) are the same as (a), but selection criteria of F_{multi} in (b) is less than 30 %, (c) is less than 40 %, (d) is less than 50 %, (e) is less than 60 %, respectively. (f) Cumulative distribution of the difference between CALIPSO CBH and Ceilometer CBH at two sites in 2017. Different colored lines represent the cumulative distribution at different selection criteria of F_{multi}.

https://doi.org/10.5194/acp-2020-1252
Preprint. Discussion started: 18 January 2021

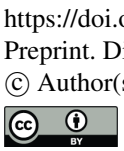

Atmospheric Chemistry and Physics Discussions

3.4.2 Cloud cover

For each 1° scene, cloud cover varies greatly. To ensure the representativeness of cloud information, one should have sufficient cloud features for the given scene, and therefore, we need to limit the minimum cloud fraction of the scene. We use the F_{cloud} to represent the cloud cover of a given 1° CALIPSO scene. For that scene, F_{cloud} is calculated using Eq. (2):

$$F_{cloud} = N_{cloud}/N_{total}, \quad (2)$$

N_{cloud} is the number of the CALIPSO lidar profiles that contains clouds (including single-layer clouds and multilayer clouds), and N_{total} is the total number of the CALIPSO lidar profiles collected in that given 1° CALIPSO scene. The sensitivity test result of F_{cloud} is displayed in Figure 6. We can see that when F_{cloud} > 10 %, the CALIPSO-retrieved CBH and ceilometer-measured CBH have the highest consistency (minimum RMSE, optimal R). Therefore, when there is too little cloud in a scene (F_{cloud} < 10 %), in order to guarantee the effectiveness of CBH retrieval, the scene is rejected.

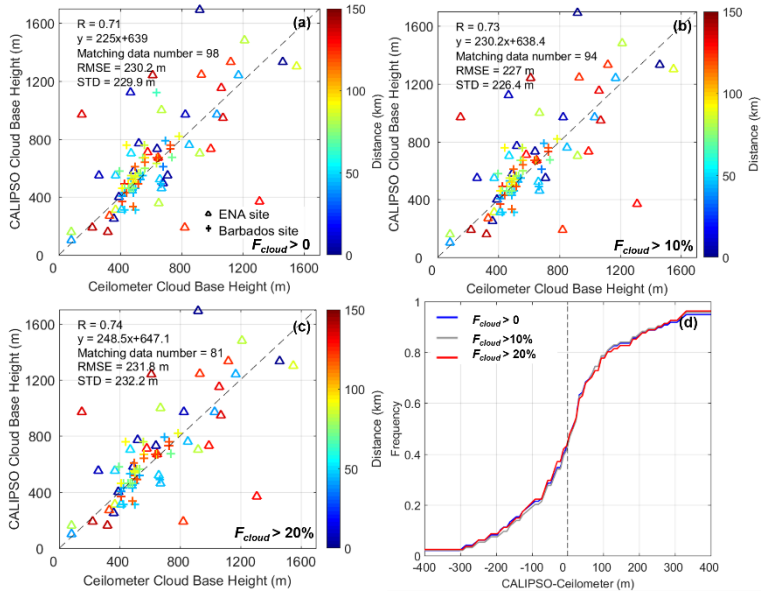

Figure 6: (a) Scatter plot of CALIPSO CBH (when cloud fraction (F_{cloud}) of one scene is equal to zero, we reject this scene; selection criteria of multilayer cloud fraction is the same as Figure 5c) and ceilometer CBH at two sites in 2017. The triangle represents the data for the ENA site, and the crosses represent the data for the Barbados site. The color represents the shortest distance from the CALIPSO ground track to the ceilometer site. (b) and (c) are the same as (a), but selection criteria of F_{cloud} in (b) is more than 10 %, (c) is more than 20 %, respectively. (d) Cumulative distribution of the difference between CALIPSO CBH and Ceilometer CBH at two sites in 2017. Different colored lines represent the cumulative distribution at different selection criteria of F_{cloud}.

3.4.3 Penetration efficiency of CALIOP

When the clouds are sufficiently thick, CALIOP lidar beam cannot penetrate them and reach the surface. Although we can use the cloud base information of thin clouds as a proxy for the cloud base of optically thicker clouds within the field, we still need to consider the penetration efficiency of CALIPSO to thick clouds. The fraction of cloudy pixels in which the lidar penetrate the clouds all the way to their base is defined as lidar penetration efficiency (E_{lidar}). E_{lidar} was used to determine what extent the lowest penetration efficiency can still provide real cloud base information in this study, which is calculated using Eq. (3):

https://doi.org/10.5194/acp-2020-1252
Preprint. Discussion started: 18 January 2021

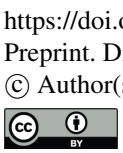

Atmospheric Chemistry and Physics Discussions

$$E_{lidar} = N_{surface\_333}/N_{total\_333}, \quad (3)$$

$N_{surface\_333}$ refers to the number of CALIPSO lidar profiles that both have 333-m horizontal resolution clouds and the detectable surface, N_{total_333} is the total number of CALIPSO lidar profiles that detected the 333-m horizontal resolution clouds. The sensitivity test result of E_{lidar} is displayed in Figure 7. We can see that the higher E_{lidar} the better cloud base height retrieval we can get, but when E_{lidar} approaches 1 we lose the ability of detecting CBH of optically thick clouds. Therefore, an optimal E_{lidar} of 50 % was chosen. That is, when the E_{lidar} < 50 % in a scene, in order to guarantee the effectiveness of CBH retrieval, the scene is rejected.

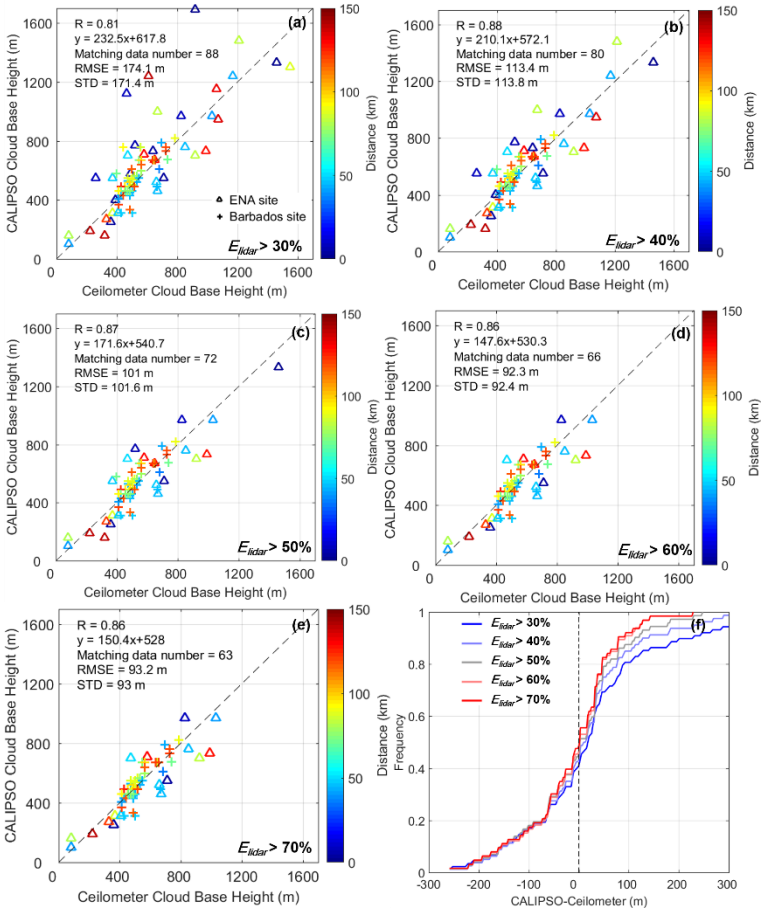

Figure 7: (a) Scatter plot of CALIPSO CBH (when penetration efficiency of 333-m horizontal resolution cloud features (E_{lidar}) of one scene is larger than 30 %, we select this scene; selection criteria of multilayer cloud fraction and cloud fraction is the same as Figure 6b) and ceilometer CBH at two sites in 2017. The triangle represents the data for the ENA site, and the crosses represent the data for the Barbados site. The color represents the shortest distance from the CALIPSO ground track to the ceilometer site. (b), (c), (d) and (e) are the same as (a), but selection criteria of E_{lidar} in (b) is larger than 40 %, (c) is larger than 50 %, (d) is larger than 60 %, (e) is larger than 70 %, respectively. (f) Cumulative distribution of the difference between CALIPSO CBH and Ceilometer CBH at two sites in 2017. Different colored lines represent the cumulative distribution at different selection criteria of E_{lidar}.

Therefore, after we obtained the initial CBH (H_{min} at 10 % quantile), we reject a 1° CALIPSO scene when:

(a) The multilayer cloud fraction of this scene is greater than 40 % (F_{multi} >40 %);

https://doi.org/10.5194/acp-2020-1252
Preprint. Discussion started: 18 January 2021

Atmospheric Chemistry and Physics Discussions

(b) Cloud fraction of this scene is less than 10 % (F_{cloud} <10 %);

(c) Penetration efficiency of CALIOP lidar of 333-m horizontal resolution cloud features is less than 50 % (E_{lidar} <50 %).

(d) If the minimum CBH of the scene is obtained at an unpenetrated cloud profile, that lowest H_{min} is updated as the final CBH of that scene.

After the above processing, we obtained the final CBH of that CALIPSO 1° scene. Then 333-m resolution cloud information as described in Section 3.1 was applied to retrieve the CTH of this scene. For all water cloud layers with a resolution of 333-m, when the CBH of low-level clouds is retrieved, we obtain the cloud top height of all 333-m cloud profiles (H_{max}) in this scene, and take the mean height of the highest 10 percentile of H_{max} as the CTH of that scene according to the definition in Zhu et al. (2018). Finally, the CGT of this 1° scene is the difference between CTH and CBH (Scheirer and Macke, 2003).

4 Evaluation of CALIPSO-retrieved CBH

In this study, we used ceilometer-measured CBH data from two ground observation stations at oceanic sites in low and mid latitude (Barbados site and ENA site) in 2017 to obtain sufficient data for the validation experiment of CALIPSO CBH retrieval. Finally, 72 sets of matching cases were obtained in 2017, including 22 matching cases for ENA site and 50 for Barbados site. The statistical analysis of these matching cases (Figure 8a) shows that, the CALIPSO-retrieved CBH has a good consistency with the CBH observed by the ceilometers at these two observation stations. The R is 0.87, the RMSE is only 101.6 m and the standard deviation (STD) is 102.2 m. Due to the restrictions of terrain and wind directions for CALIPSO scenes in ENA site as described in Section 2.2, the ENA site matches fewer cases than the Barbados site in 2017. The cumulative distribution of the CBH difference between CALIPSO and ceilometer in Figure 8b indicates that ~70 % of the matching cases have a deviation of less than 100 m.

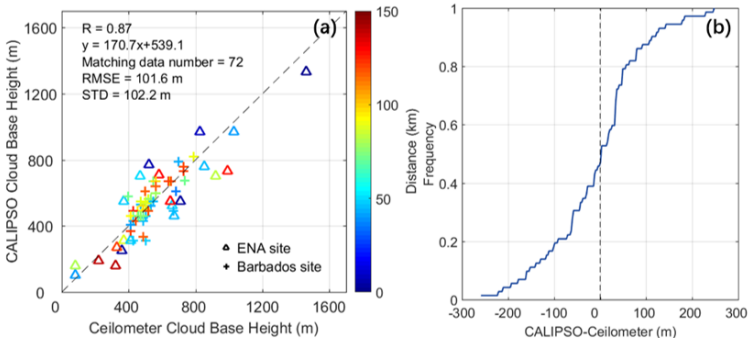

Figure 8: (a) Scatter plot of CALIPSO CBH and ceilometer CBH at two sites in 2017. The triangle represents the data for the ENA site, and the crosses represent the data for the Barbados site. The color represents the shortest distance from the CALIPSO ground track to the ceilometer site. (b) Cumulative distribution of the difference between CALIPSO CBH and Ceilometer CBH at two sites in 2017.

https://doi.org/10.5194/acp-2020-1252
Preprint. Discussion started: 18 January 2021


Atmospheric Chemistry and Physics Discussions

5 Global distributions

5.1 Overall distributions

Based on the above retrieval methodology, we further obtained the global geographic distribution of annual mean CBH, CTH and CGT on a 2° × 2° latitude–longitude grids in 2014 and 2017 (Figure 9). To ensure the validity of the retrieval results, we only use the data at a 2-degree grid when there are more than 20 valid scenes on this grid, among which the valid scenes indicates that we have retrieved the CBH, CTH and CGT based on the 333-m resolution cloud data. Therefore, CALIPSO data in 2014 were also applied in this study to ensure most the grids have sufficient valid scenes to produce the global distribution. The blanks in the geographic distribution are mainly due to the lack of valid scenes for a given grid. This is more frequent over land than over ocean, because there are more scenes with lots of optical thicker clouds and multilayer clouds over land.

The CBH distribution (Figure 9a) shows most CBHs above surface in the land area are higher than over ocean. In the oceanic area, the cloud bases are higher in the mid-latitudes than at the equatorial regions and at high latitudes, which are in well agreement with Mülmenstädt et al. (2018). In addition, in the mid-latitudes, the lowest cloud bases are mostly concentrated in offshore areas (Böhm et al., 2019), which are mainly less than 400 m. The clouds with large CTHs are mainly distributed in the ocean area at low and high latitudes and the land area, mainly over 2,000 m, which are consistent with the result of Sun-Mack et al. (2014). Similar to the distribution of the CBH, the smallest CTHs are also concentrated in offshore areas and the equatorial regions of the western hemisphere, which are mainly ~1,000 m, in agreement with Zuidema et al. (2009). Thus, shallow clouds with small CGTs (<800 m) mainly distributed at the mid latitude oceanic area and offshore areas with a percentage of ~10 %. These areas mainly include the west coast areas of South America, Africa, the United States, and Australia, and are equally high-incidence areas of stratocumulus clouds (Wood, 2012). That will be helpful to future studies of marine stratocumulus microphysics and aerosol-cloud interaction. Moreover, thick clouds with large CGTs are mainly located in the tropics and in the mountainous regions, such as the western Pacific and the Rocky Mountains of western Canada.

https://doi.org/10.5194/acp-2020-1252
Preprint. Discussion started: 18 January 2021

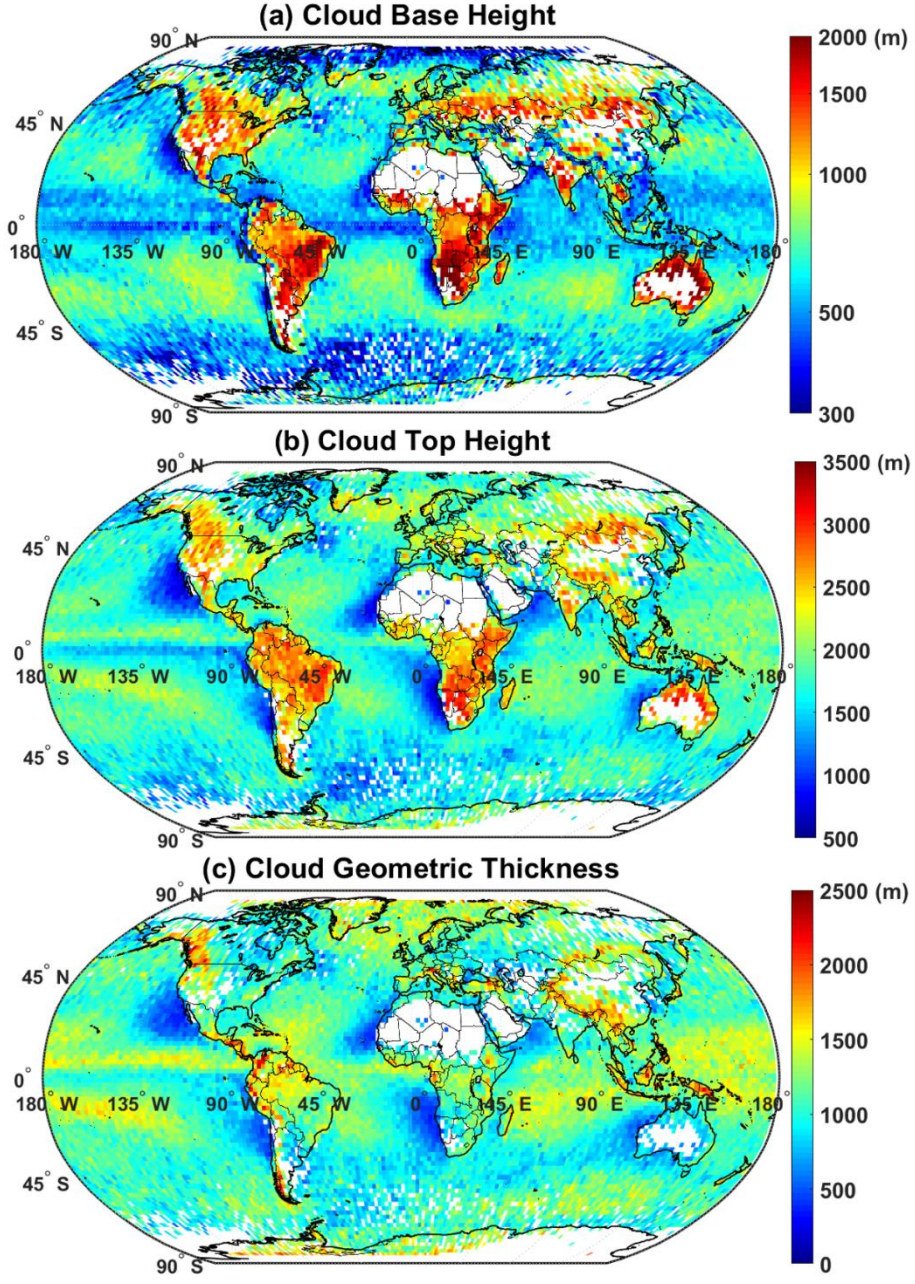

Figure 9: Geographic distributions of annual mean CBH, CTH and CGT on a 2° × 2° latitude–longitude grid in 2014 and 2017. The heights are in m above ground level.

In addition, we obtained the geographic distribution of CTH and CGT by taking the maximum value of H_{max} as the CTH of each 1° CALIPSO scene (as showed in Figure A2). The spatial distribution of CTH/CGT in Figures A2a and A2c is similar to the distribution of CTH/CGT by using the mean height of the highest 10 percentile of H_{max} as the CTH (Figures 9b and 9c). However, the cumulative distribution of the difference (Figure A2d) indicates that the CGT based on the maximum value of

https://doi.org/10.5194/acp-2020-1252
Preprint. Discussion started: 18 January 2021

Atmospheric Chemistry and Physics Discussions

H_{max} is larger than that based on the mean height of the highest 10 percentile of H_{max}, ~66 % of cases have difference less than 100 m. The maximum difference reached 300 m, with ~3 % greater than 200 m. Those areas with high differences are concentrated in the oceans at low latitudes, which are mainly convective clouds.

5.2 Seasonal distributions

The seasonally averaged geographic distributions of CBH, CTH and CGT (Figures 10, 11 and 12) are generally consistent with the distributions of the annual averaged results (Figure 9), but are influenced by the variation of convective intensity in different seasons, and also exhibit some unique seasonal characteristics. The CBH and CTH over land in the mid-latitude Northern Hemisphere are much greater in June-July-August (JJA) than other seasons and lowest in December-January-February (DJF). The mid-latitude global oceans have the lowest CBH (mostly below 500 m), CTH and CGT in summer seasons, and the highest cloud top height in winter, while the CBH, CTH and CGT distribution reversed over high-latitude Southern Oceans. Previous study also shown the same seasonal pattern of CBH and CTH distributions (Böhm et al., 2019), but with minimum discernible CBH > ~700 m.

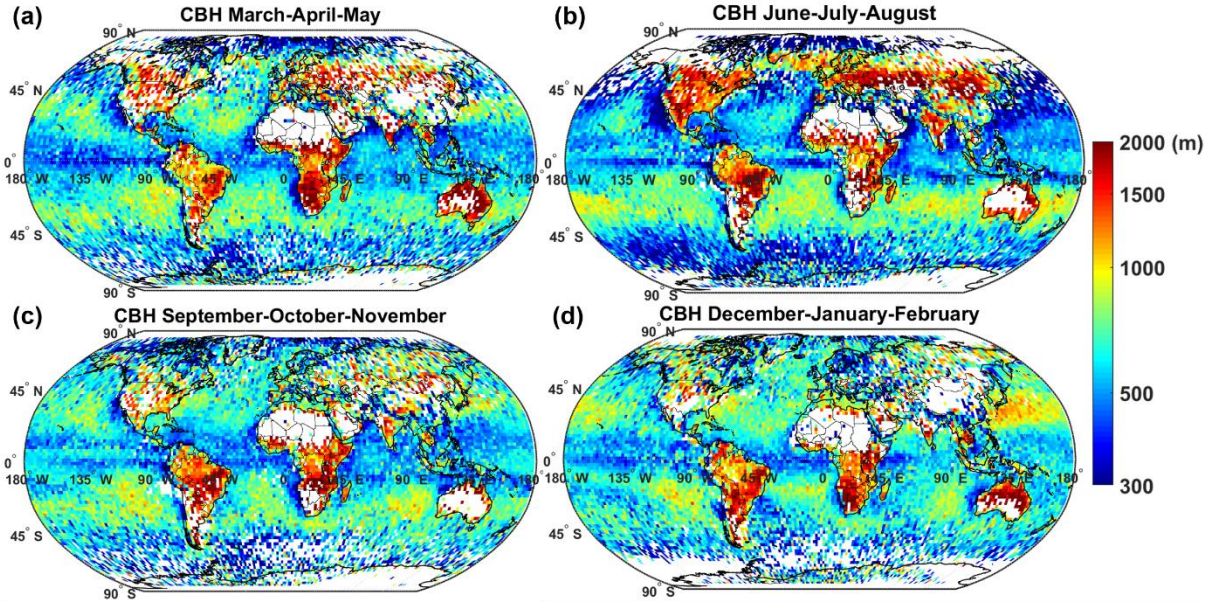

Figure 10: Geographic distributions of seasonal averaged CBH on a 2° × 2° latitude–longitude grid in 2014 and 2017. (a) March, April and May; (b) June, July and August; (c) September, October, and November; (d) December, January, and February. The heights are in m above ground level. Each grid has at least 5 valid scenes.

https://doi.org/10.5194/acp-2020-1252
Preprint. Discussion started: 18 January 2021

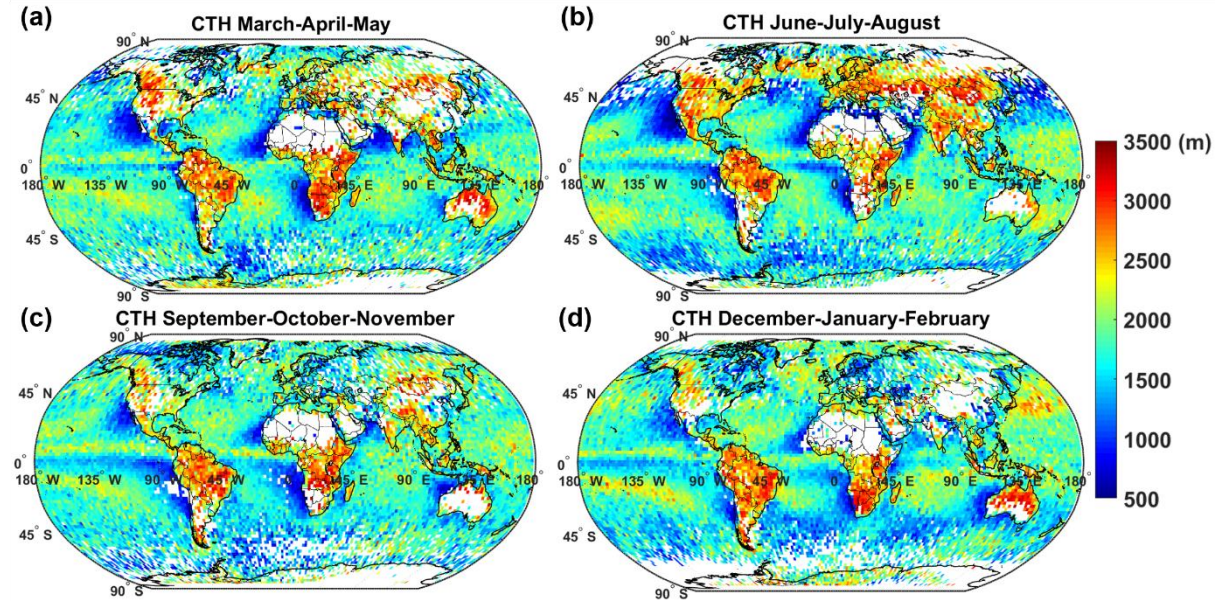

Figure 11: The same as Figure 10, but for CTH.

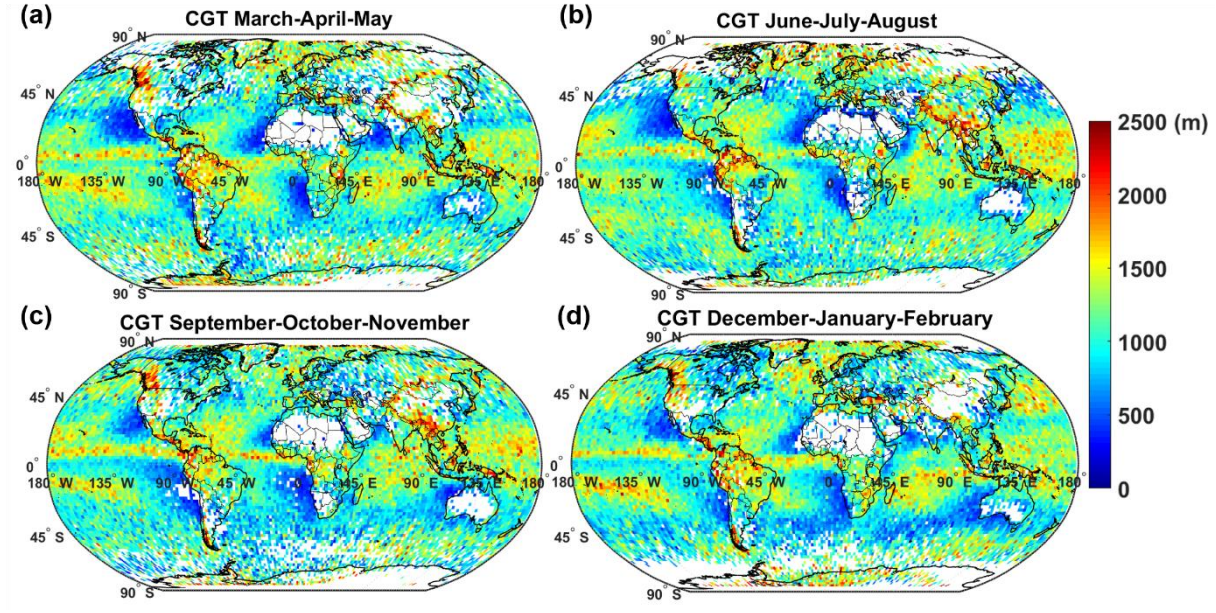

Figure 12: The same as Figure 10, but for CGT.

To further investigate the spatial variation of the cloud geometry information over land and ocean with different seasons, we plotted the mean meridional distribution maps (Figure 13). Regional variations in CBH and CTH are more pronounced over land than over the ocean during all seasons. The CTH follows CBH, especially over land. The seasonal variations are smaller

https://doi.org/10.5194/acp-2020-1252
Preprint. Discussion started: 18 January 2021

Atmospheric Chemistry and Physics Discussions

over ocean, and CBH and CTH show the maximum variations at the winter subtropical latitudes and the summer mid-latitudes, respectively. An equatorial minimum occurs in all seasons.

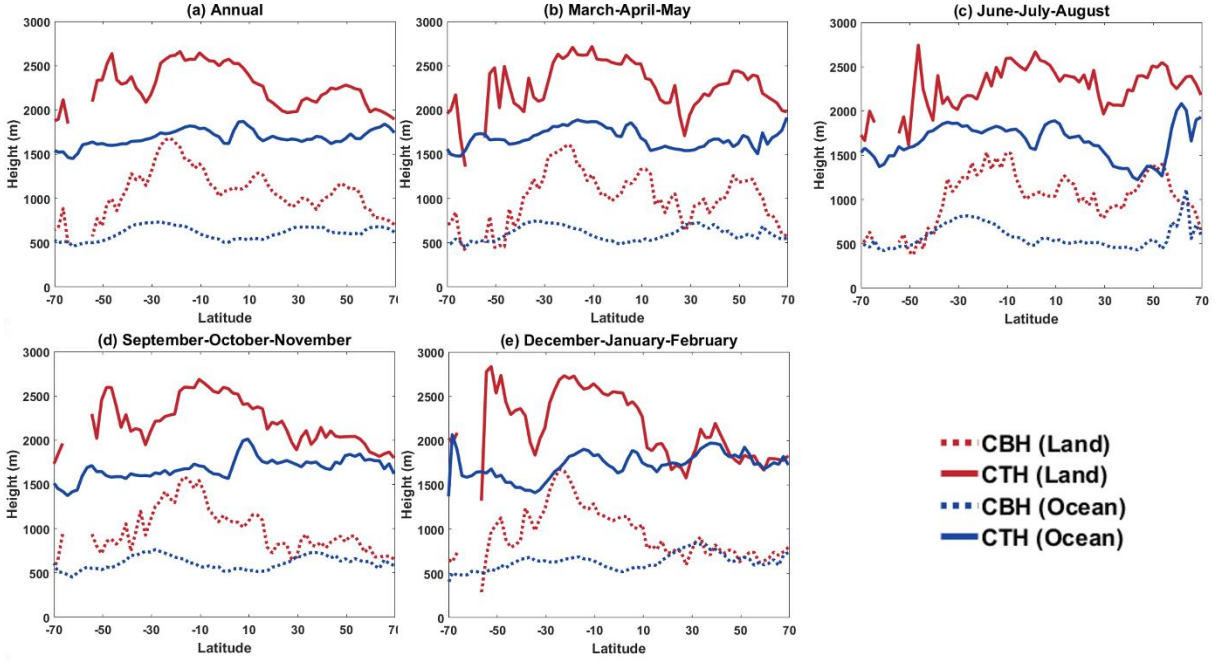

Figure 13: Mean meridian CBH and CTH annual and seasonal distributions. Straight lines indicate CTH, and dotted lines indicate CBH (ocean in blue, land in red). (a) Annual; (b) March, April and May; (c) June, July and August; (d) September, October, and November; and (d) December, January, and February.

5.3 Diurnal distributions

For the comparison of day-time and night-time distributions, we further obtained the diurnal geographical and mean meridional distributions of CBH and CTH in Figure 14. More boundary layer clouds occur over land during the day-time than at night-time at middle and low latitudes, as evident by the sparse coverage on the geographic distribution maps. This means that either there are less clouds during night, or the clouds become multilayer or obscured by deep or high clouds. The opposite is true for the Southern Oceans region. Overall, the CTHs over land are much higher during the day-time than at night-time, while over ocean they are opposite, night-time has slightly higher CTH than day-time by ~300 m as shown by the meridional mean distributions. The CBH over land is greater during day-time than at night-time, but over ocean the CBH is consistent both day-time and night-time. The difference of CTH and CBH between land and ocean is greater during day-time than at night-time, especially the CTH.

https://doi.org/10.5194/acp-2020-1252
Preprint. Discussion started: 18 January 2021

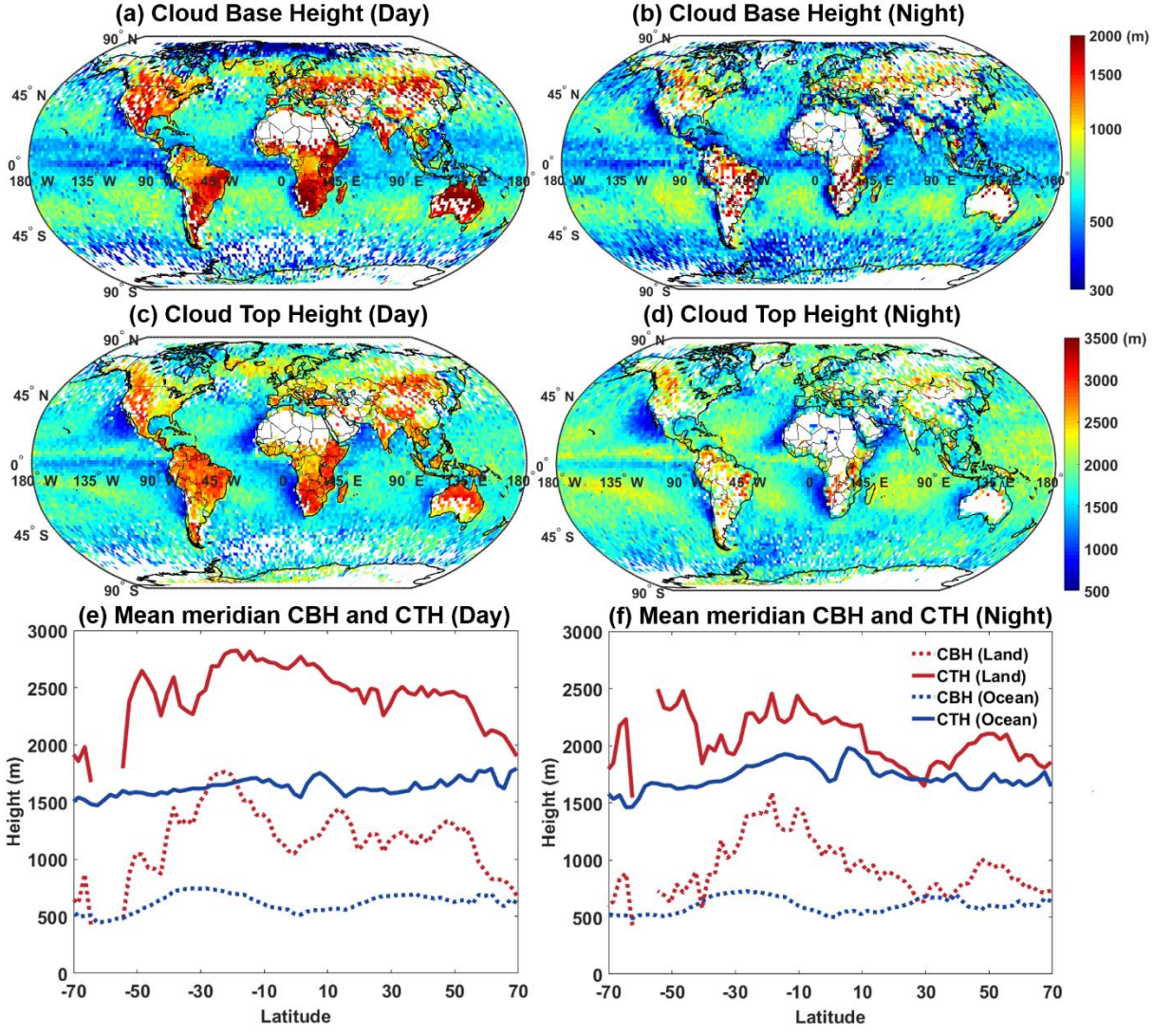

Figure 14: (a) Geographic distributions of annual mean CBH on a 2° × 2° latitude–longitude grid in 2014 and 2017 for CALIPSO day-time; (b) is the same as (a), but for night-time; (c) is the same as (a), but for CTH; (d) is the same as (c), but for night-time. The heights are in m above ground level. Each grid has at least 10 valid scenes. (e) Mean meridian CBH and CTH over land and the ocean for CALIPSO day-time. Straight lines indicate CTH, and dotted lines indicate CBH (ocean in blue, land in red). (f) is the same as (e), but for night-time.

6 Discussion

The CBH retrieval methodology in this study has been greatly improved compared to other current satellite CBH retrieval algorithms. According to the geographic distribution maps (Figure 9) generated from the high-accuracy CBH, CTH and CGT data in this study, we find the following features that can be further discussed:

https://doi.org/10.5194/acp-2020-1252
Preprint. Discussion started: 18 January 2021


Atmospheric Chemistry and Physics Discussions

i. **The effect of SST on CBH and CGT.** The patterns show the obviously higher CBH over land compared to ocean, especially over the arid areas. Shallow and thin clouds prevail over cool sea surface temperatures (SST) to the west of subtropical coastlines, and thicken gradually westward. The CBH increases faster than CGT with the distance from land in these regions. The thickest clouds occur over the regions with highest SST, such as the tropical west Pacific. A conspicuous narrow strip of clouds with low CBH and CGT is noted over the Equator, most notably over the eastern half of the Pacific Ocean. This feature is the manifestation of the equatorial ocean upwelling and cooling in response to the poleward flow of surface water in response to the easterly stress by the winds (Adam, 2020).

ii. **High base and thick clouds over tropical basins.** CBH is lowest near the shores of South America, Namibia, Western Australia and southern North America, because of the flow of warm continental air over the cold sea surface, which creates a strong inversion above it. This, in fact, leads to formation of low cloud decks near the sea surface. This effect is weakening with distance from the shore. Therefore, these coastal regions are dominated by stratocumulus clouds, with CBH mainly below ~400 m and increasing up to ~900 m far from the continent (the detailed distribution of CBH of the Southeast Atlantic is shown in Figure 15a). In contrast, Böhm et al. (2019) could only derive a minimum CBH of ~700 m and therefore could not resolve cloud base information of marine stratocumulus clouds. Moreover, over the tropical basins, such as the Amazon Basin and the Congo Basin, clouds developed high and thick with CBH larger than 1000 m and CGT larger than 1500 m (the detailed distribution of CBH of the Congo Basin is shown in Figure 15b), which responds to strong convective motion in the tropics (Sun-Mack et al., 2014). In contrast, the CGT and CBH in this region was only about 500 and 700 m, respectively, in the study of Böhm et al. (2019), which are similar to their retrieval of the marine stratocumulus region as described above.

iii. **Large CGT and small CBH over the Southern Oceans.** CBH is quite low over the low SST of the Southern Oceans, but CGT is much larger there than over the eastern margins of the subtropical oceans. The lowering of CBH towards Antarctica in the Southern Oceans is caused by the more frequent and stronger thermal inversions at high latitudes (Li et al., 2013), with CBH largely below 500 m. This is much lower than the ~800 m CBH in the Southern Oceans inferred in previous studies (Böhm et al., 2019).

iv. **Low and thick clouds over the Maritime Continent.** CBH increases rapidly over inland of tropical Africa, America and Australia, while keeping CGT little changed. The CBH increases much less over the Maritime Continent. Convection develops vigorously over those land areas, resulted in large CGT mainly greater than 1500 m, whereas the surrounding ocean area CGT<1500 m (the detailed distribution of CGT of the Maritime Continent is shown in Figure 15c).

v. **Orographic clouds.** Mountain ranges in Western Canada, Mexico, the southern Himalayas, and central New Guinea have a low cloud base, but significantly larger CGT than the surrounding areas. It is primarily caused by orographic lifting of the air masses, resulting in adiabatic cooling and condensation to form cloud droplets (Miller et al., 2018), which increase the CTH over these mountainous regions, which results in large CGT (the detailed distribution of CGT of the southern Himalayas is shown in Figure 15d).

https://doi.org/10.5194/acp-2020-1252
Preprint. Discussion started: 18 January 2021

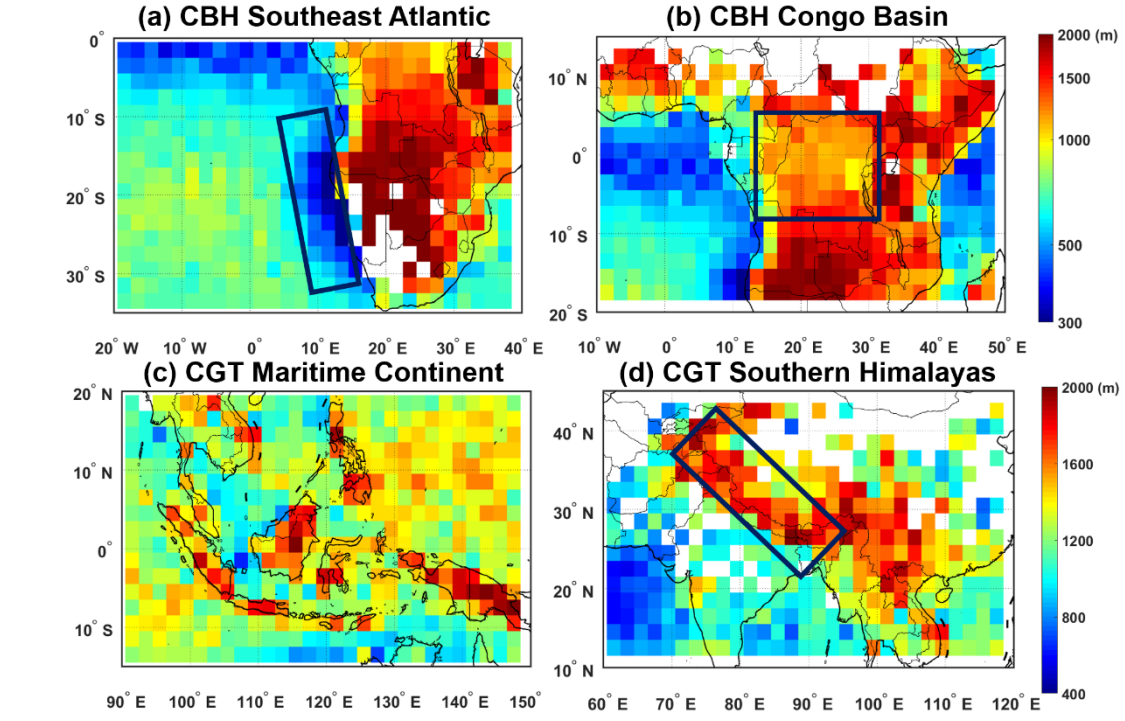

Figure 15: Geographic distributions on a 2° × 2° latitude–longitude grid in 2014 and 2017. (a) CBH over the Southeast Atlantic; (b) CBH over the Congo Basin; (c) CGT over the Maritime Continent; (d) CGT over the southern Himalayas. The heights are in m above ground level. The dark blue boxes represent the location of the regions of interest.

7 Conclusions

Based on the highest resolution VFM data of CALIPSO lidar observations, a new methodology for retrieving the CBH, CTH and CGT of low-level clouds is proposed. This methodology uses the 333-m resolution water cloud distribution of VFM data to retrieve CBH with superior performance. The methodology can effectively reduce the interference to CBH retrieval due to surface signal, multilayer cloud and boundary layer aerosols. Moreover, even when the thickness of the cloud is sufficient to fully attenuate the CALIPSO lidar signal, the method provides an accurate CBH by taking the CBH of the surrounding thinner cloud as representative of the entire cloud field. At the same time, the retrieval of CBH, CTH and CGT within 1° scenes along the CALIPSO track as the statistical range reduces the influence of the cloud anvils on the retrieval of CBH. The methodology was tested and validated based on two in situ ceilometer measurements in 2017. The linear correlation coefficient is 0.87, and an error standard deviation is ±100 m. This high-precision CBH retrieval methodology developed in this study is a great improvement over other current satellite CBH retrieval methods with RMSE of several hundred meters or even several km. Based on this methodology, we obtained the annual, seasonal and diurnal distributions of global CBH, CTH and CGT for two years. The lowest cloud base/top heights are both concentrated in eastern margins of the oceans in the subtropical latitudes. A

https://doi.org/10.5194/acp-2020-1252
Preprint. Discussion started: 18 January 2021

Atmospheric Chemistry and Physics Discussions

narrow band of lower clouds occurs along the Equator. Seasonal analysis showed that differences in CBH and CTH were more pronounced over land than over the ocean. The seasonal variation of CBH and CTH is greater in the Northern Hemisphere than in the Southern Hemisphere, both over land and over the ocean. The diurnal distribution suggests that CTH is much higher over land during the daytime than at night-time, while this phenomenon is mirrored and much weaker over ocean. This high-precision cloud geometry information also shows several interesting features: (1) there are noticeable differences in cloud geometry characteristics between the eastern and western parts of the Pacific Ocean; (2) high base and thick clouds occur over tropical basins; (3) the lowering of CBH towards Antarctica in the Southern Oceans, while deepening CGT; (4) low and thick clouds occur over the Maritime Continent; (5) increased CGT over mountains.

Accurate CBH information is of great significance for evaluating the cloud coupling state and its relevance to the effects of aerosols on cloud cover (Goren et al., 2018). The result in this study can also be applied to understanding the cloud microphysical processes and improve the accuracy of cloud radiation feedback in the numerical model (Hartmann, 2009;Jian et al., 2006;Merk et al., 2016;Viúdez-Mora et al., 2015). However, we can only retrieve CGT by leaving out the high multilayer cloud fraction and low penetration efficiency of CALIPSO VFM data. Therefore, the current method cannot deal with CALIPSO scenes with a large amounts of multilayer clouds and non-penetration optical thick clouds.

Appendix A

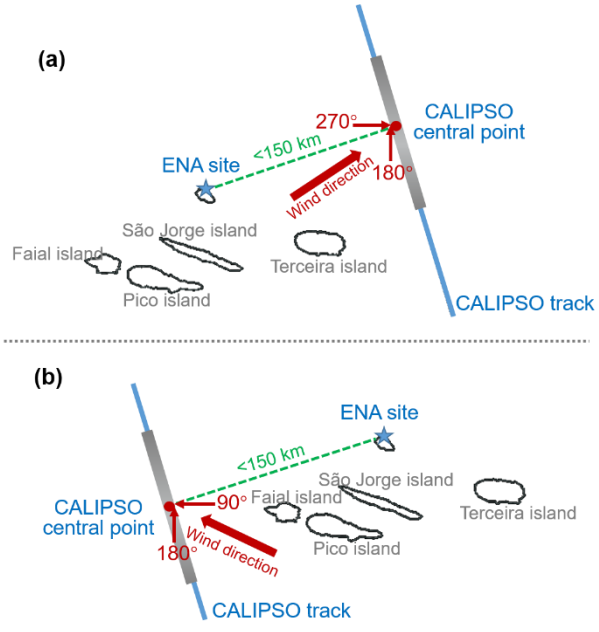

Figure A1: Schematic of matching between the CALIPSO and the ENA observation site. The blue pentagram indicates the location of ceilometer site, the blue line is the CALIPSO track, the red circle represents the CALIPSO central point, the dashed green line represents the shortest distance from the site to the CALIPSO central point, the grey shade area is the 1° CALIPSO scene, and the

https://doi.org/10.5194/acp-2020-1252
Preprint. Discussion started: 18 January 2021

Atmospheric Chemistry and Physics Discussions

red arrow represents the wind direction of the CALIPSO data. (a): CALIPSO track is located at the east ocean of ENA site. Wind directions of rejected CALIPSO data: 180-270°. (b): CALIPSO track is located at the west ocean of ENA site. Wind directions of rejected CALIPSO data: 90-180°.

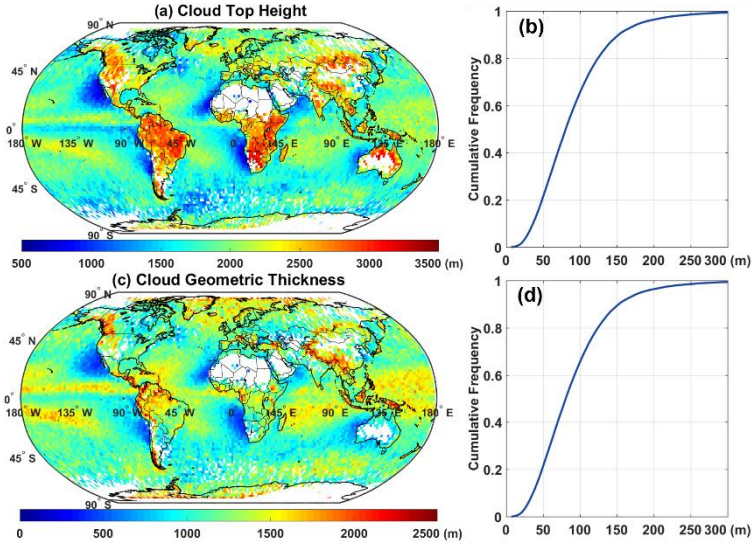

Figure A2: (a) Geographic distribution of CTH based on the maximum value of H_{max} on a 2°× 2° latitude–longitude grid in 2014 and 2017. (b) Cumulative distribution of the difference between the CTH based on the maximum value of H_{max} and CTH based on the mean height of the highest 10 percentile of H_{max} in 2014 and 2017. (c)/(d) is the same as (a)/(b), but for CGT. The heights are in m above ground level.

Data availability: The CALIPSO VFM data used in this study can be downloaded from https://search.earthdata.nasa.gov/search/granules?p=C1556717896-LARC_ASDC&tl=1578270083!4 (last access: October 2020), Atmospheric Radiation Measurement ceilometer observation data are obtained from https://adc.arm.gov/discovery/#/results/site_code::ena/meas_category_code::cloud/meas_subcategory_detail::cloud.macro (last access: October 2020) and Barbados Cloud Observatory data are available at https://www.mpimet.mpg.de/en/science/the-atmosphere-in-the-earth-system/working-groups/tropical-cloud-observation/barbadosstation1/instrumentation-and-data/ (last access: October 2020).

Author contribution: DR conceived the study. XL, YZ and DR designed the cloud base height and geometric thickness retrieval methodology. XL implemented the methodology and carried out the data analysis with help from YZ and FM. ZP,

FM and WG provided useful comments on the paper. XL prepared the manuscript with contributions from YZ, DR and the other co-authors.

Competing interests: The authors declare that they have no conflict of interest.

Acknowledgements: This work was supported by the National Natural Science Foundation of China (41971285, 41627804, and 42075093), the National Key Research and Development Program of China (2018YFC1507903), and the Fundamental Research Funds for the Central Universities (2042019kf0192). We are grateful to the science teams for providing excellent and accessible CALIPSO, Atmospheric Radiation Measurement ceilometer observation and Barbados Cloud Observatory data.

References

Adam, O.: Dynamic and energetic constraints on the modality and position of the intertropical convergence zone in an aquaplanet, J. Climate, 1-53, doi:10.1175/JCLI-D-20-0128.1, 2020.

Böhm, C., Sourdeval, O., Mülmenstädt, J., Quaas, J., and Crewell, S.: Cloud base height retrieval from multi-angle satellite data, Atmos. Meas. Tech., doi:10.5194/amt-12-1841-2019, 2019.

Baker, N.: Joint Polar Satellite System (JPSS) VIIRS cloud base height algorithm theoretical basis document (ATBD), JPSS Ground Project Code, 474-00045. 2011.

Burton, S. P., Ferrare, R. A., Vaughan, M. A., Omar, A. H., Rogers, R. R., Hostetler, C. A., and Hair, J. W.: Aerosol classification from airborne HSRL and comparisons with the CALIPSO vertical feature mask, Atmos. Meas. Tech., 12(5):1397-1412, doi:10.5194/amt-6-1397-2013, 2013.

Dupont, J. C., Haeffelin, M., Morille, Y., Comstock, J. M., Flynn, C., Long, C. N., Sivaraman, C., and Newson, R. K.: Cloud properties derived from two lidars over the ARM SGP site, Geophys. Res. Lett., 38, 99-106, doi: 10.1029/2010GL046274, 2011.

Efraim, A., Rosenfeld, D., Schmale, J., and Zhu, Y.: Satellite Retrieval of Cloud Condensation Nuclei Concentrations in Marine Stratocumulus by Using Clouds as CCN Chambers, J. Geophys. Res.-Atmos., 125, doi:10.1029/2020JD032409, 2020.

Fan, C., Wang, M., Rosenfeld, D., Zhu, Y., Liu, J., and Chen, B.: Strong Precipitation Suppression by Aerosols in Marine Low Clouds, Geophys. Res. Lett., 47, doi:10.1029/2019gl086207, 2020.

Fan, J., Wang, Y., Rosenfeld, D., and Liu, X.: Review of Aerosol–Cloud Interactions: Mechanisms, Significance, and Challenges, J. Atmos. Sci., 73, 4221-4252, doi:10.1175/jas-d-16-0037.1, 2016.

Goren, T., Rosenfeld, D., Sourdeval, O., and Quaas, J.: Satellite Observations of Precipitating Marine Stratocumulus Show Greater Cloud Fraction for Decoupled Clouds in Comparison to Coupled Clouds, Geophys. Res. Lett., doi:10.1029/2018GL078122, 2018.

Grosvenor, Daniel, P., Field, Paul, R., Hill, Adrian, A., and Shipway: The relative importance of macrophysical and cloud albedo changes for aerosol-induced radiative effects in closed-cell stratocumulus: insight from the modelling of a case study, Atmos. Chem. Phys., doi:10.5194/acp-17-5155-2017, 2017.

Grosvenor, D. P., and Wood, R.: The effect of solar zenith angle on MODIS cloud optical and microphysical retrievals within marine liquid water clouds, Atmos. Chem. Phys., 14, 7291-7321, doi:10.5194/acp-14-7291-2014, 2014.

Hahn, C. J., Rossow, W. B., and Warren, S. G.: ISCCP Cloud Properties Associated with Standard Cloud Types Identified in Individual Surface Observations, J. Climate, 14, 11-28. 2001.

Hartmann, D. L.: Understanding the Importance of Microphysics and Macrophysics for Warm Rain in Marine Low Clouds. Part II: Heuristic Models of Rain Formation, J. Atmos. Sci., 66, 2973-2990, doi:10.1175/2009jas3072.1, 2009.

Huo, J., Lu, D., Duan, S., Bi, Y., and Liu, B.: Comparison of the cloud top heights retrieved from MODIS and AHI satellite data with ground-based Ka-band radar, Atmos. Meas. Tech., 13, 1-11, doi:10.5194/amt-13-1-2020, 2020.

Jian, Y., Qiang, F., and Mcfarlane, N.: Tests and improvements of GCM cloud parameterizations using the CCCMA SCM with the SHEBA data set, Atmos. Res., 82, 0-238, doi:10.1016/j.atmosres.2005.10.009, 2006.

Kyle, E., Fitch, Keith, D., Hutchison, Kevin, S., Bartlett, and Robert: Assessing VIIRS cloud base height products with data collected at the Department of Energy Atmospheric Radiation Measurement sites: International Journal of Remote Sensing: Vol 37, No 11, Int. J. Remote Sens., doi:10.1080/01431161.2016.1182665, 2016.

https://doi.org/10.5194/acp-2020-1252
Preprint. Discussion started: 18 January 2021

Atmospheric Chemistry and Physics Discussions

Lenaerts, J. T., Gettelman, A., Van Tricht, K., van Kampenhout, L., and Miller, N. B.: Impact of Cloud Physics on the Greenland Ice Sheet Near-Surface Climate: A Study With the Community Atmosphere Model, J. Geophys. Res.-Atmos., 125, doi:10.1029/2019JD031470, 2020.

Li, J. M., Yi, Y. H., Stamnes, K., Ding, X. D., Wang, T. H., Jin, H. C., and Wang, S. S.: A new approach to retrieve cloud base height of marine boundary layer clouds, Geophys. Res. Lett., 40, 4448-4453, doi:10.1002/grl.50836, 2013.

Mülmenstädt, J., Sourdeval, O., Henderson, D. S., L'Ecuyer, T. S., and Quaas, J.: Using CALIOP to estimate cloud-field base height and its uncertainty: The Cloud Base Altitude Spatial Extrapolator (CBASE) algorithm and dataset, Earth. Syst. Sci. Data., 10, 2279-2293, doi:10.5194/essd-10-2279-2018, 2018.

Mace, G. G., and Zhang, Q.: The CloudSat radar-lidar geometrical profile product (RL-GeoProf): Updates, improvements, and selected results, J. Geophys. Res.-Atmos., 119, 9441-9462, doi:10.1002/2013JD021374, 2014.

Merk, D., Deneke, H., Pospichal, B., and Seifert, P.: Investigation of the adiabatic assumption for estimating cloud micro- and macrophysical properties from satellite and ground observations, Atmos. Chem. Phys., 16, 933-952, doi:10.5194/acp-16-933-2016, 2016.

Noh, Y. J., Forsythe, J. M., Miller, S. D., Seaman, C. J., Li, Y., Heidinger, A. K., Lindsey, D. T., Rogers, M. A., and Partain, P. T.: Cloud-Base Height Estimation from VIIRS. Part II: A Statistical Algorithm Based on A-Train Satellite Data, J. Atmos. Oceanic Technol., 34, 585-598, doi:10.1175/JTECH-D-16-0110.1, 2017.

Rosenfeld, D., Zheng, Y., Hashimshoni, E., Pöhlker, M. L., and Andreae, M. O.: Satellite retrieval of cloud condensation nuclei concentrations by using clouds as CCN chambers, P. Natl. Acad. Sci. USA, 113, 5828-5834, doi:10.1073/pnas.1514044113, 2016.

Rosenfeld, D., Zhu, Y., Wang, M., Zheng, Y., Goren, T., and Yu, S.: Aerosol-driven droplet concentrations dominate coverage and water of oceanic low-level clouds, Science, 363, doi:10.1126/science.aav0566, 2019.

Sato, Y., and Suzuki, K.: How do aerosols affect cloudiness?, Science, 363, 580-581, doi:10.1126/science.aaw3720, 2019.

Scheirer, R., and Macke, A.: Cloud inhomogeneity and broadband solar fluxes, J. Geophys. Res.-Atmos., 108, doi:10.1029/2002JD003321, 2003.

Seaman, C. J., Noh, Y. J., Miller, S. D., Heidinger, A. K., and Lindsey, D. T.: Cloud-Base Height Estimation from VIIRS. Part I: Operational Algorithm Validation against CloudSat, J. Atmos. Oceanic Technol., 34, 567-583, doi:10.1175/JTECH-D-16-0109.1, 2017.

Seung-Hee, Ham, Seiji, Kato, Fred, G., Rose, David, Winker, and Tristan: Cloud occurrences and cloud radiative effects (CREs) from CERES-CALIPSO-CloudSat-MODIS (CCCM) and CloudSat radar-lidar (RL) products, J. Geophys. Res.-Atmos, doi:10.1002/2017jd026725, 2017.

Stephens, G. L., and Webster, P. J.: Cloud Decoupling of the Surface and Planetary Radiative Budgets, J. Atmos. Sci., 41, 681-686. 2010.

Stephens, G. L., Christensen, M., Andrews, T., Haywood, J., and Sy, O.: Cloud Physics from Space, Quart. J. Roy. Meteor. Soc., doi:10.1002/qj.3589, 2019.

Sun-Mack, S., Minnis, P., Yan, C., Kato, S., and Winker, D. M.: Regional apparent boundary layer lapse rates determined from CALIPSO and MODIS data for cloud height determination, J. Appl. Meteorol. Clim., 53, doi:10.1175/JAMC-D-13-081.1, 2014.

Twomey, S.: Pollution and the planetary albedo, Atmos. Environ. (1967), 8, 1251-1256, doi:10.1016/0004-6981(74)90004-3, 1974.

Vaughan, M. A., Winker, D. M., and Powell, K. A.: CALIOP algorithm theoretical basis document, part 2: Feature detection and layer properties algorithms, Rep. PC-SCI, 202, 87. 2005.

Viúdez-Mora, A., Costa-Surós, M., Calbó, J., and González, J. A.: Modeling atmospheric longwave radiation at the surface during overcast skies: The role of cloud base height, J. Geophys. Res.-Atmos., 120, 199-214, doi:10.1002/2014JD022310, 2015.

Weisz, E., Li, J., Menzel, W. P., Heidinger, A. K., Kahn, B. H., and Liu, C. Y.: Comparison of AIRS, MODIS, CloudSat and CALIPSO cloud top height retrievals, Geophys. Res. Lett., 34, doi:10.1029/2007GL030676, 2007.

Winker, D. M., Hunt, W. H., and Mcgill, M. J.: Initial performance assessment of CALIOP, Geophys. Res. Lett., 34, doi: 10.1029/2007GL030135, 2007.

Winker, D. M., Vaughan, M. A., Omar, A., Hu, Y., Powell, K. A., Liu, Z., Hunt, W. H., and Young, S. A.: Overview of the CALIPSO Mission and CALIOP Data Processing Algorithms, J. Atmos. Oceanic Technol., 26, 2310-2323, doi: 10.1175/2009JTECHA1281.1, 2009.

Wood, R.: Stratocumulus clouds, Mon. Wea. Rev., 140, 2373-2423, doi:10.1175/mwr-d-11-00121.1, 2012.

Zhao, S., and Suzuki, K.: Differing Impacts of Black Carbon and Sulfate Aerosols on Global Precipitation and the ITCZ Location via Atmosphere and Ocean Energy Perturbations, J. Climate, 32, doi:10.1175/JCLI-D-18-0616.1, 2019.

Zheng, Y., and Rosenfeld, D.: Linear relation between convective cloud base height and updrafts and application to satellite retrievals, Geophys. Res. Lett., 42, 6485-6491, doi:10.1002/2015GL064809, 2015.

Zheng, Y.: Theoretical Understanding of the Linear Relationship between Convective Updrafts and Cloud-Base Height for Shallow Cumulus Clouds. Part I: Maritime Conditions, J. Atmos. Sci., 76, 2539-2558, doi:10.1175/jas-d-18-0323.1, 2019.

Zheng, Y., Sakradzija, M., Lee, S.-S., and Li, Z.: Theoretical Understanding of the Linear Relationship between Convective Updrafts and Cloud-Base Height for Shallow Cumulus Clouds. Part II: Continental Conditions, J. Atmos. Sci., 77, 1313-1328, doi:10.1175/jas-d-19-0301.1, 2020.

Zhu, Y., Rosenfeld, D., Yu, X., Liu, G., Dai, J., and Xu, X.: Satellite retrieval of convective cloud base temperature based on the NPP/VIIRS Imager, Geophys. Res. Lett., 41, 1308-1313, doi:10.1002/2013GL058970, 2014.

Zhu, Y., Rosenfeld, D., and Li, Z.: Under what conditions can we trust retrieved cloud drop concentrations in broken marine stratocumulus?, J. Geophys. Res.-Atmos., 123, 8754-8767, doi:10.1029/2017JD028083, 2018.

https://doi.org/10.5194/acp-2020-1252
Preprint. Discussion started: 18 January 2021

Atmospheric Chemistry and Physics Discussions

Zuidema, P., Painemal, D., De Szoeke, S., and Fairall, C.: Stratocumulus Cloud-Top Height Estimates and Their Climatic Implications, J. Climate, 22, 4652-4666, doi:10.1175/2009JCLI2708.1, 2009.

550